communications earth & environment

A Nature Portfolio journal

Article

https://doi.org/10.1038/s43247-025-02407-w

Green roofs act as the first barrier to intercept microplastics from urban atmosphere

Check for updates

Jianshi Huang[1], Mengrong Bao[1], Shuangqi Wu[1], Ying Wang[2] & Shuiping Cheng[1,3]

Green roofs are often considered barriers against polluted precipitation, but their effectiveness in capturing airborne microplastics remains unclear. Here we evaluate modular green roofs under simulated wet deposition to assess their ability to intercept and retain microplastics. We find that green roofs remove over 97.5% of deposited microplastics. In Shanghai, China, this corresponds to an annual interception of approximately 1.70×10^{12} particles, or 56.2 tonnes. Higher rainfall intensity slightly improves capture efficiency by increasing moisture and reducing infiltration forces. Fragment-shaped microplastics are more easily retained than fiber-shaped ones. Most particles are trapped in the soil layer, while some are retained by vegetation, although air turbulence may remobilize fibers. Surface and chemical analysis reveals that plastic materials within green roofs themselves can degrade, potentially releasing microplastics in the process. These results show that green roofs can play a valuable role in reducing urban microplastic pollution and offer practical insights for designing future stormwater and air-quality management strategies.

Microplastic pollution has become pervasive across aquatic[1,2], terrestrial[3,4], and atmospheric ecosystems[5,6], raising escalating global concerns. The proliferation of these particles is closely linked to human activities, posing a latent risk to human health[7,8]. In coastal cities, the transport of microplastics involves a complex exchange of substances between the ocean, inland areas, and urban environments. The primary pathways for microplastics into coastal urban landscapes include atmospheric deposition, stormwater transport, riverine input, and marine wave action, with both atmospheric fallout and stormwater runoff serving as significant entry and transport mechanisms[5,9,10]. This deposition not only facilitates the entry of microplastics into aquatic systems but also increases the potential for human inhalation exposure[11].

In efforts to mitigate urban atmospheric microplastic deposition, research has increasingly focused on the efficacy of surface runoff treatment facilities. Systems such as bioretention ponds[12], vegetated swales[13], and constructed wetlands[14] have demonstrated commendable capabilities in intercepting microplastics horizontally. These facilities may also contribute to treating microplastics from roof runoff, although their efficiency in this regard requires further investigation. However, the input of microplastics from atmospheric deposition remains significant even after interception[15], underscoring the necessity for further research on reducing this atmospheric input.

Urban rooftops, as primary receptors for both atmospheric wet and dry deposition, provide a strategic opportunity for the initial interception of atmospheric pollutants. Over the past decade, research on green roofs as modifications of impermeable rooftops has accelerated. There is substantial evidence that these sustainable practices provide multiple environmental benefits, including air cleaning, stormwater retention, and runoff purification[16], thereby reducing the burden on local water treatment facilities. However, previous studies on green roofs have primarily focused on the reducing dissolved matters such as nutrients, heavy metals, and organic pollutants[17,18], with little attention given to atmospheric particulates like microplastics. Since roof areas constitute 40–50% of urban impermeable areas[19], developing green roofs holds significant potential for intercepting atmospheric microplastic and improving urban water quality, warranting further investigation.

This study employed a green roof module as a pilot installation to evaluate its ability in intercepting microplastics under various rainfall conditions. By investigating the vertical transport mechanisms of atmospheric microplastic within green roof systems during wet deposition, this research aimed to elucidate the underlying processes and dynamics. The

[1]Key Laboratory of Yangtze River Water Environment, Ministry of Education, Institute of Eco-environmental Engineering, College of Environmental Science and Engineering, Tongji University, 200092 Shanghai, PR China. [2]Key Laboratory of National Forestry and Grassland Administration on Ecological Landscaping of Challenging Urban Sites, Shanghai Academy of Landscape Architecture Science and Planning, 200232 Shanghai, PR China. [3]Shanghai Institute of Pollution Control and Ecological Security, 200092 Shanghai, PR China. e-mail: shpcheng@tongji.edu.cn

findings were expected to enhance our understanding of microplastic transport in urban environments and inform strategies to prevent the transfer of atmospheric microplastic pollution into aquatic ecosystems.

Results and discussion

Temporal dynamics of microplastics during rainfall events and interception flux

Effluent microplastic concentrations from green roofs were tracked during simulated rainfall events. As shown in Fig. 1, concentrations generally ranged from dozens to hundreds, decreasing over time since the onset of outflow. Notably, microplastic concentrations dropped within the first 20 min, reaching levels 2–5 times higher than those in later stage of rainfall. This pattern is likely due to the limited retention capacity of the green roof substrate and the direct input of MPs from precipitation, rather than a typical 'first flush' effect caused by accumulated pollutants being washed off after a dry period. Unlike surface runoff systems, where first flush results from pollutant buildup during antecedent dry periods[20], the MPs concentration in our inflow remained constant across rainfall events. This suggests that the observed trend is driven by initial rapid percolation through the substrate rather than the wash-off of deposited particles. Given that green roofs typically experience cycles of wetting and drying over long-term operations[21], their internal structures and effectiveness in trapping pollutants can vary. For instance, cracks and channels may form during dry periods, facilitating preferential flow during subsequent rainfalls. This allows microplastics to pass through more readily in the initial 20 min. Additionally, while microplastics trapped in green roofs may be re-released

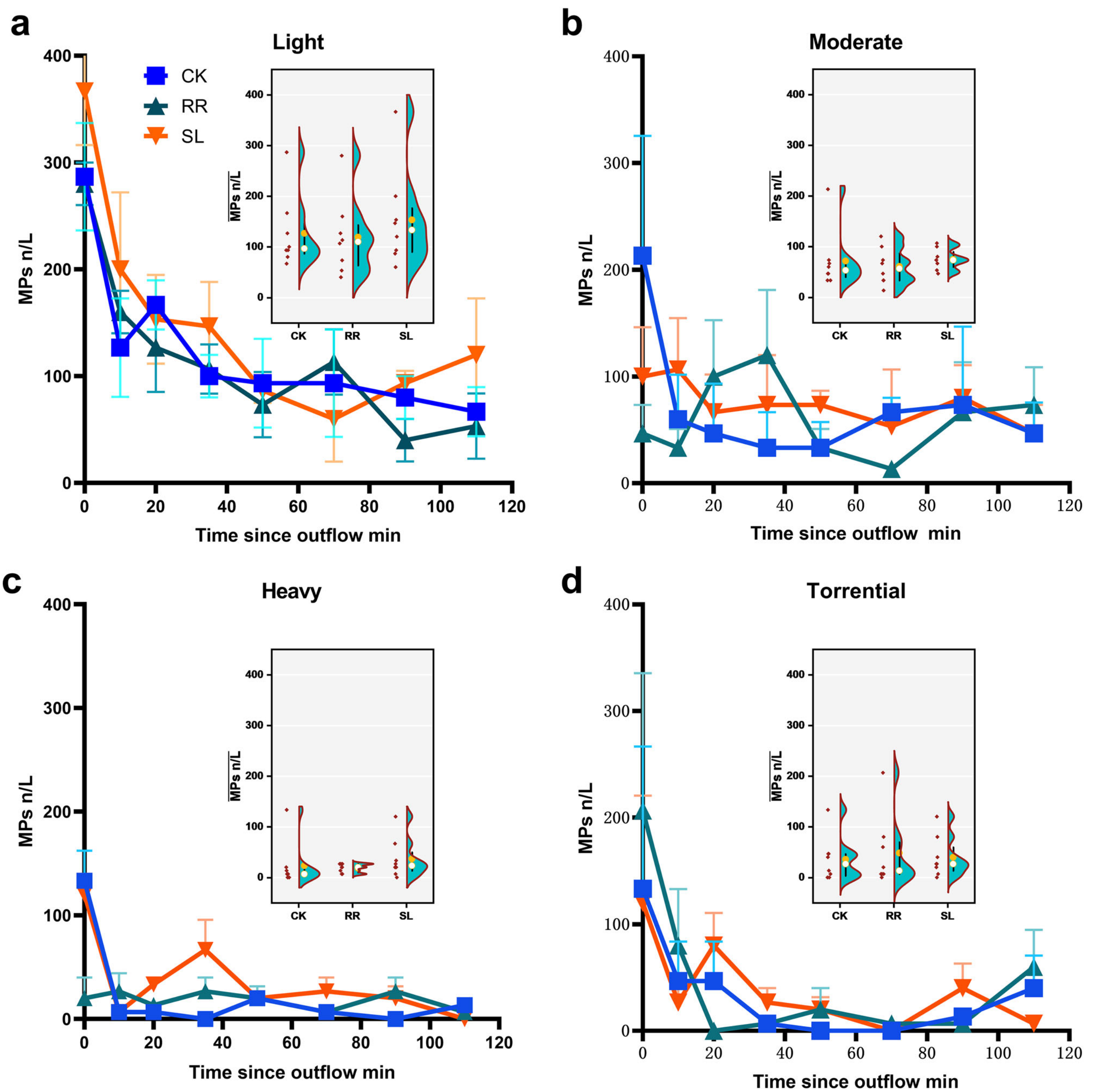

Fig. 1 | Time courses for the effluent concentration of microplastics during simulated rainfall events. **a** Light rainfall (2.5 mm h^{-1}). **b** Moderate rainfall (7.5 mm h^{-1}). **c** Heavy rainfall (14.5 mm h^{-1}). **d** Torrential rainfall (36.5 mm h^{-1}) (BL: blank group, CK: control group, RR: *R. rosea* group, SL: *S. lineare* group). Error bars represent the standard deviation of triplicate measurements. The violin plots illustrate the distribution of MPs concentrations under different treatments (CK, RR, SL) for each rainfall intensity. The kernel density function was applied to visualize the data distribution. In the plots, red dots represent individual data points, yellow circles indicate the mean values, white circles show the median values, and black vertical lines denote the interquartile range (25–75%).

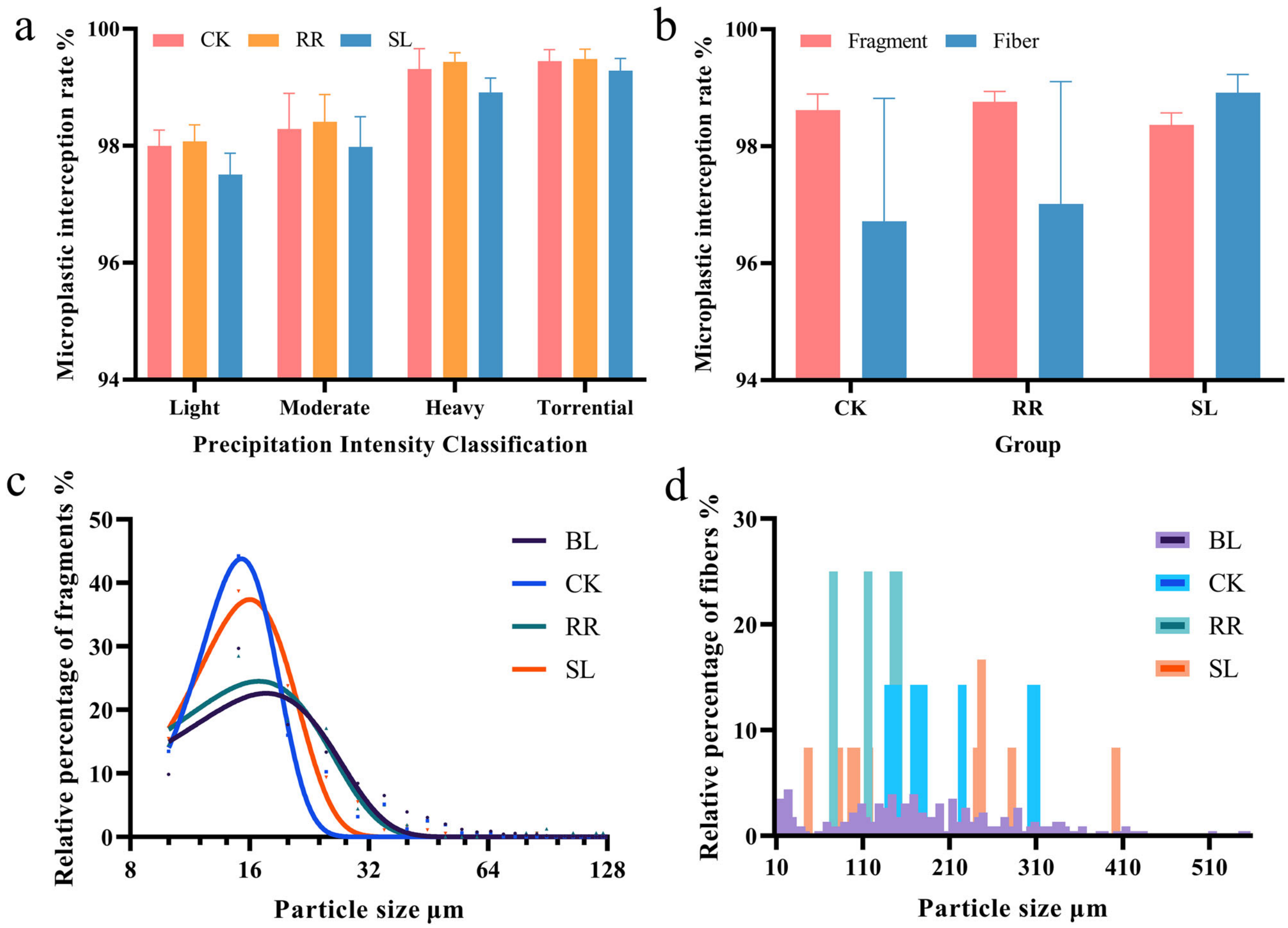

Fig. 2 | Microplastics interception efficiency of by green roofs and particle characteristics of effluent microplastics. **a** Impacts of rainfall intensity and vegetation on interception efficiency. **b** Interception efficiency variation between fragments and fibers. **c** Particle size distribution of effluent fragments. **d** Particle size distribution of effluent fibers. (BL: blank group, CK: control group, RR: *R. rosea* group, SL: *S. lineare* group). Error bars represent the standard deviation of triplicate measurements.

during subsequent precipitation events, this effect appears to be relatively weak and may depend on factors such as rainfall intensity, substrate retention capacity, and microplastic particle characteristics (e.g., size and density). The observed trend is illustrated in Fig. S1, highlighting the variability across different rainfall events. Consequently, the preferential flow induced by antecedent drying can lead to high effluent microplastic concentrations early in rainfall.

Each treatment demonstrated an average microplastic interception rate of over 97.5% in simulated rainfall events (Fig. 2a), indicating the efficacy of green roof modules in capturing and filtering out atmospheric microplastics during wet depositions. On a citywide scale in Shanghai, China, the annual interception flux of microplastics by green roofs was estimated. Currently, Shanghai has ~3.56 million m^2 of green roofs, according to data from the Shanghai Greening and Amenity Administration (https://lhsr.sh.gov.cn). The average microplastic abundance in precipitation is estimated at 368 $n\,L^{-1}$[22], and the city's annual rainfall over the past 5 years averages 1334 mm, according to the Shanghai Municipal Water Affairs Bureau. Accordingly, the annual flux of atmospheric microplastics intercepted by green roofs in Shanghai is estimated to exceed 1.70×10^{12} $n\,yr^{-1}$, assuming a minimum interception efficiency of 97.5% as presented in Fig. 2a. Converting this to a weight-based value using a unit weight of 3.3×10^{-5} $g\,n^{-1}$[23], the flux is ~56.2 $t\,yr^{-1}$—1.65 times higher than the annual microplastic input from domestic wastewater into urban water bodies (34.0 $t\,yr^{-1}$)[24]. Thus, the expansion and implementation of green roofs on regional and city scales have considerable potential to reduce atmospheric microplastic pollution cost-effectively, underscoring their importance and value in sustainable development.

It is important to note that this estimation is based on controlled experimental conditions and does not universally represent the efficiency of all green roofs in Shanghai. In practice, green roof performance may vary due to differences in roof inclination, substrate composition, plant selection, and local climate conditions. Additionally, temporal variations such as seasonal weather patterns and prolonged droughts may influence the hydrological and filtration processes of green roofs, potentially affecting their interception efficiency. While our study provides a preliminary estimate, further large-scale field investigations are necessary to refine these calculations and better understand the variability of green roof performance in real-world settings.

Factors influencing interception efficiency and underlying contributors

Four types of rainfall events, categorized by intensity (2.5, 7.0, 14.5, and 36.5 $mm\,h^{-1}$), were used to examine the variability of effluent microplastics under different precipitation scenarios (Fig. 1). The highest microplastic concentrations were observed during light rainfall events, ranging from 40 to 367 $n\,L^{-1}$. In contrast, heavier precipitations presented lower microplastic concentrations, representing 13–213 $n\,L^{-1}$ for moderate, 0–133 $n\,L^{-1}$ for heavy, and 0–207 $n\,L^{-1}$ for the torrential one. Interestingly, recent studies have found a positive correlation between rainfall intensity and microplastic concentration in stormwater runoff, where increasing intensity dislodges settled microplastics from impermeable surfaces[25]. However, the surface of green roof is permeable, and the infiltration process may dominate the effluent microplastic concentration.

The interception efficiency of microplastics under different rainfall intensities was further calculated and analyzed. An increase in interception efficiency was observed with higher precipitation intensity (Fig. 2a). For example, the average interception efficiency enlarged from 97.5% for light precipitation to 99.4% for torrential precipitation ($P < 0.05$). Green roofs appear more effective at filtering out microplastics and preventing their downstream transport under higher rainfall intensities. This may be due to increased rainfall intensity enhancing the vertical impact of raindrops, which compacts the loose soil to a greater extent. Therefore, the firmer soil reduces the size of pores and channels, creating stronger steric hindrance to microplastic migration. This may explain the relatively higher interception efficiency observed during heavier rainfall scenarios.

The selection of plant species is a crucial aspect of green roof development, as the longevity of the roof depends significantly on plant health[16]. In this study, two plant species commonly used for green roofs in Shanghai, *R. rosea* (RR) and *S. lineare* (SL), were selected to examine their effectiveness in enhancing stormwater quality. As shown in Fig. 1, the effluent microplastic concentrations in unplanted treatment (CK) were slightly lower than those in the planted treatments (i.e., RR and SL). For instance, during the torrential precipitation, the mean microplastic concentration was 35.8 n L^{-1} for CK, while 40.0 n L^{-1} for RR and 48.3 n L^{-1} for SL. Although no significant difference was observed between the unplanted and planted treatments ($P > 0.05$), the interception efficiency of the treatment SL was slightly lower than that of CK and RR across all rainfall scenarios (Fig. 2a). Despite the plants in urban green infrastructures have been known to aid in the removal of dissolved matters such as nutrients and heavy metals[26], their role in removing particulate matters like TSS or microplastics might be different.

It has been reported that both the physical and chemical properties of the planting medium can be altered by the root growth[27], affecting stormwater infiltration and the transport of associated substances. For example, plant roots can squeeze the substrate through mechanical actions such as extension, thickening and interpenetration, creating fissures and channels that increase substrate porosity[28]. These root-growth-induced features may lead to preferential stormwater flow and the movement of associate particles like microplastics[29], accelerating their infiltration. In treatment SL, observations during plant sample collection revealed that the root system was more extensive compared to RR, with a dense network of lateral roots forming a well-developed fibrous structure. This root-induced alteration in substrate porosity likely facilitated the migration of microplastics by creating additional preferential flow channels, ultimately leading to lower interception efficiency. In contrast, the treatment CK was unplanted, thus represented a slightly higher removal efficiency.

Fragments and fibers demonstrated variations in interception efficiency by green roof. As shown in Fig. 2b, fragments exhibited slightly higher removal efficiency than fibers in both CK and RR treatments, with efficiencies of 98.6% and 98.5%, respectively, compared to 96.7% and 97.0% for fibers. Similar findings have been reported in bioretention systems used to remove microplastics from urban stormwater. The elongated shape of fibers allows them to pass through smaller pores or channels where fragments are typically trapped, increasing their proportion from 79% at the inlet to 94% at the outlet[25]. Likewise, thinner fiber diameters result in deeper infiltration depths in glass sphere columns, which simulate natural sediment, whereas fragments infiltrate less deeply due to entanglement in the pores[30]. Consequently, morphology plays a notable role in the varying removal efficiencies of fibers and fragments, with narrower widths being less likely to be trapped.

Variations were also observed in the particle size distribution between fibers and fragments. In Fig. 2c, the peaks for green roof treatments (i.e., CK, RR, and SL) are narrower and shift to smaller particle sizes compared to the blank treatment (BL). This indicates the potential for green roofs to trap and filter out some microplastics in the form of fragment with large particle size. The peaks for treatments CK and SL were particularly narrowed, indicating selective capture of fragments and a concentration of uncaptured particles in smaller size intervals. In contrast, fibers exhibit different particle size distribution patterns. As shown in Fig. 2d, fibers in green roof treatments are concentrated in specific particle sizes but are distributed discontinuously, making Gaussian fitting of their distribution curves more challenging compared to fragments. This suggests that fibers are captured more selectively by green roofs in terms of particle size, resulting in effluent concentrations at specific sizes.

In addition, parameters such as spherical diameter equivalent, perimeter, roundness (similarity to a circle), aspect ratio, solidity (ratio of convex envelope area to surface area), and surface area of outflow microplastics were analyzed and Gaussian fitted (Fig. S2). Differences were observed between green roof treatments and BL treatment in each parameter. In particular, the peaks of spherical diameter equivalent and surface area in treatments CK and SL were narrower and shifted to smaller directions compared to treatment BL. These variations are similar to those observed for fragment particle size distribution (Fig. 2c), suggesting that fragments may have a greater impact on the variation in microplastic diameter distribution than fibers.

The infiltration rate is a critical variable affecting the process of particle migration in soil or sediment and is closely related to the variations in rainfall intensity and matrix hydraulic property[31]. One key factor influencing hydraulic properties is soil moisture content, which has been shown to dominate over other factors[32]. Hence, moisture content and infiltration time (the duration from stormwater injection to discharge within green roofs) were monitored in green roof treatments under different rainfall events. As shown in Fig. 3a, the moisture contents of planted treatments RR and SL were significantly higher than in the unplanted CK treatment during all rainfall events. This is expected, as plants are known to improve water-holding capacity and increase stormwater retention in urban green infrastructures[33]. Their root networks helped retain infiltrated water. Increasing rainfall intensity from light to moderate significantly enlarged the moisture contents in all treatments, although further increases to heavy or torrential rainfall did not result in significant changes. The limited depth (40 mm) of planting soil layer may be responsible, leading to a saturation of soil moisture during moderate precipitation. In addition, infiltration time of each treatment was recorded simultaneously (Fig. 3b). The infiltration times for planted treatments RR and SL were significantly longer than that for CK during the light precipitation. The higher moisture content in RR and SL may explain this, as previous studies have shown that higher soil moisture reduces infiltration rates and prolongs infiltration time[34]. Likewise, a positive correlation between soil moisture content and infiltration time was observed[31], but this correlation was limited once the soil layer became saturated. RR and SL treatments presented similar infiltration time to CK during moderate, heavy, and torrential events due to saturation. Another factor influencing infiltration time was rainfall intensity, which decreased infiltration time as intensity increased, likely due to the increased initial velocity of raindrops.

Quantifying how microplastics are captured by soil pores, cracks, and channels during stormwater infiltration is complex. We propose the concept of a “water network” to clarify this process using soil moisture content (Fig. 3c). Increased moisture content densifies and swells the water network, creating more cross-linked infiltration pathways within the soil layer. This can serpentine the water flow and prolong the infiltration time, thus diminishing the hydraulic gradient and decreasing the driving force responsible for water infiltration[35]. On the other hand, increased moisture content can cause clay particles to swell, shrinking the porous structure of soil and further reducing corresponding hydraulic gradient[36]. A lower hydraulic gradient implies more resistances and head losses for stormwater and the associated particles like microplastics. Here the treatment RR retained more moisture in soil (Fig. 3a), accounting for its relatively higher microplastics interception efficiency than SL (Fig. 2a). Likewise, increased rainfall intensity raised the moisture content (Fig. 3a), reducing the hydraulic gradient and enhancing microplastic interception efficiency (Fig. 2a).

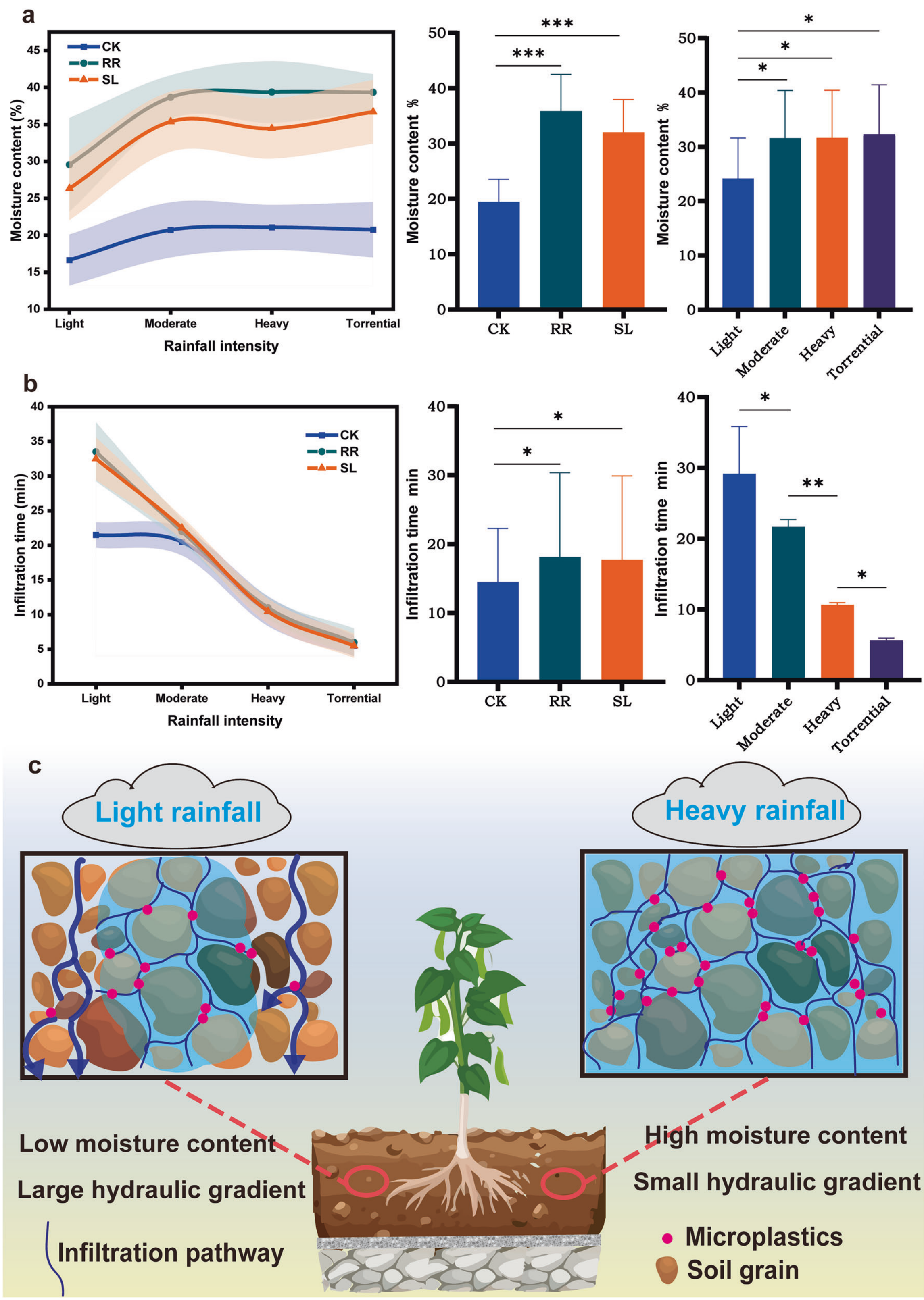

Fig. 3 | Effects of rainfall intensity and vegetation on the hydraulic property of the planting soil layer in green roofs. a Moisture content variation. **b** Infiltration time variation. **c** Schematic of the infiltration process affected by the proposed contributor. Specifically, the thick lines represent relatively larger preferential flow channels that exist under low soil moisture conditions, allowing for faster infiltration. In contrast, the thin lines correspond to finer channels formed due to soil swelling under higher moisture conditions, resulting in slower infiltration (BL: blank group, CK: control group, RR: *R. rosea* group, SL: *S. lineare* group). Error bars and shading represent the standard deviation of triplicate measurements.

Principal component analyses (PCA) and advanced correlation link were performed to further understand how specific climate variables and configuration setup affect the capture of microplastics (Fig. 4). Variables include "*d*" (MP particle diameter), "*s*" (solidity), "out" (outflow concentration), and "ssa" (specific surface area). Fiber.re, fragment.re, and MPs.re denote the removal efficiency of fiber-type, fragment-type, and total microplastics, respectively. Apparently, the presence of vegetation altered the correlation patterns, resulting in a more concentrated distribution (Fig. 4a and b). This suggests that the correlations among these parameters were stronger in planted treatments compared to CK. For example, in the CK treatment, the fragment.re and fiber.re were distributed evenly on both sides of MPs.re, indicating similar contributions to the overall removal efficiency of microplastics. However, the PCA analysis revealed that in the planted treatments, fragment.re was positioned closer to MPs.re compared to fiber.re (Fig. 4b). This suggests that fragment removal followed a similar pattern to overall MPs removal, whereas fiber removal deviated from this trend. Additionally, the Pearson correlation coefficient for fragment.re increased from 0.91 (CK) to 0.97 (planted treatments), while fiber.re decreased from 0.72 to −0.22 (Fig. 4c and d). This shift indicates that vegetation enhanced the consistency of fragment retention with total MPs retention but disrupted the removal pattern of fibers, implying a preferential retention of fragments. This phenomenon may be attributed to differences in microplastic shape and interaction with vegetation. Fragments, being more compact and irregular in shape, are likely to become physically trapped within plant structures (e.g., root zones, stems, and soil pores), where they experience reduced mobility[25]. In contrast, fibers are more elongated and flexible, which may allow them to move more freely within water pathways and bypass interception by substrates[30]. Additionally, a mantel test revealed more significant correlations between climate variables and effluent water parameters in planted treatments. This indicates the potential of vegetation to respond to climate variations and impact the infiltration process.

Spatial distribution of microplastics within the green roof module

The distribution of microplastics within the green roof facility was analyzed by counting the number of microplastics trapped in each component (Fig. 5a). The planting soil layer dominated in microplastic interception (66.2–92.2%), with the vegetation layer (defined as the overground part of plants) playing a secondary role. Notably, the vegetation layer in treatment SL contributed 24.4% to microplastic capture, compared to just 9.1% in treatment RR. This difference may be attributed to the distinct leaf structures of the SL and RR plants. As shown in Fig. S3, SL's leaves are tufted and denser than those of RR, providing a larger surface area for trapping microplastics—881.6 n cm^{-2} for SL versus 374.6 n cm^{-2} for RR. However, this contribution was negligible for fibers, with no significant difference observed between SL and RR. Fibers have a larger specific surface area compared to fragments, making them more susceptible to air turbulence, which can lead to their re-suspension and re-entry into the atmosphere. This phenomenon accounts for a higher percentage of microplastics classified as "other". The contributions from the root zone (0–1.0%), drainage aquifer (1.1–2.4%), and isolation filter layer (0–0.03%) were minimal and can be considered negligible.

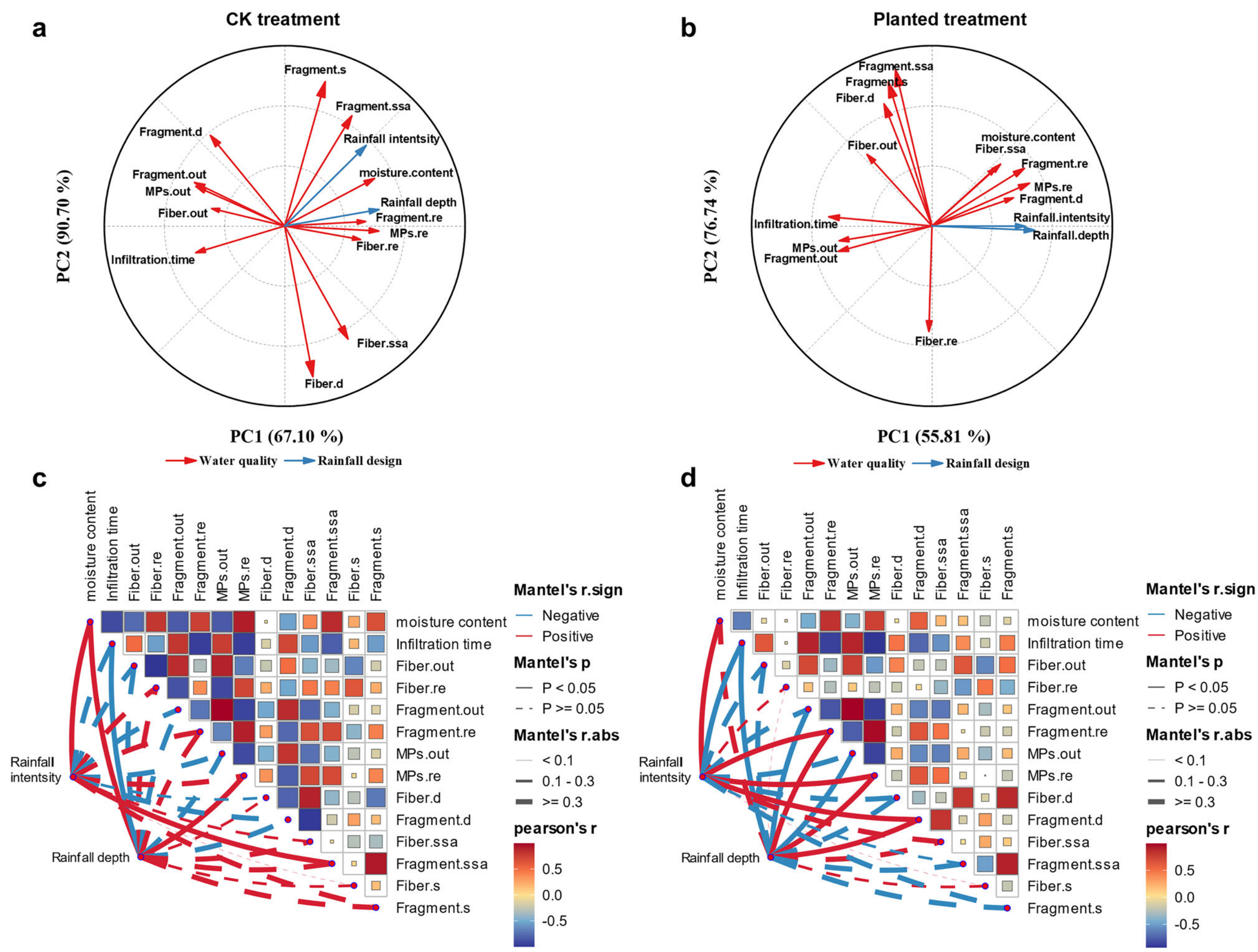

Fig. 4 | Principal component analyses (PCA) and advanced correlation link between climate variables and green roof effluent parameters. a PCA analysis for treatment CK. **b** PCA analysis for planted treatments (RR and SL). **c** Correlation link for treatment CK. **d** correlation link for treatment planted treatments. Solid line: significant, $p < 0.05$; dash line: non-significant, $p > 0.05$ (CK: control group, RR: *R. rosea* group, SL: *S. lineare* group).

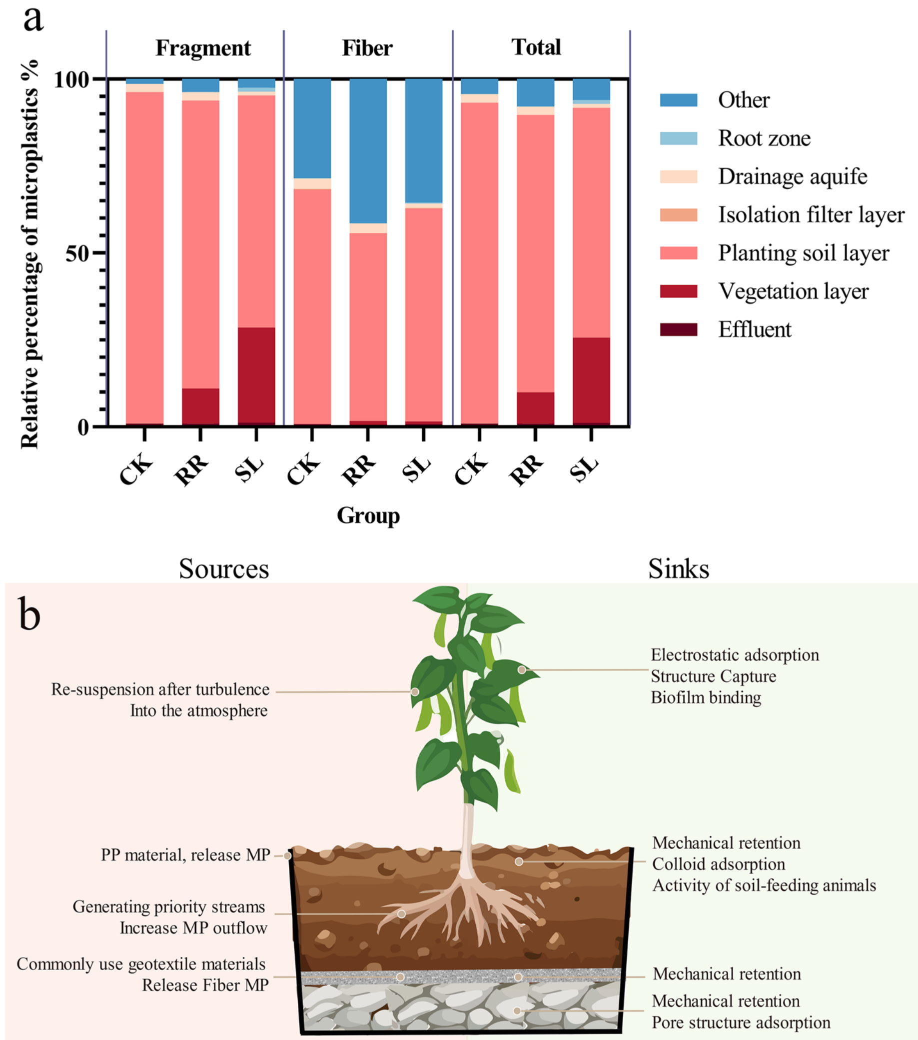

Fig. 5 | Spatial distribution of microplastics trapped within green roofs. **a** Contribution of each green roof component to microplastic trapping. **b** Schematic of source–sink analysis of microplastics within green roof modules (CK: control group, RR: *R. rosea* group, SL: *S. lineare* group).

The interception mechanism of microplastics by green roof was proposed in Fig. 5b and each component was discussed, respectively. Plant leaves have been reported to play an important role in intercepting airborne microplastics[37]. One key factor influencing the interception efficiency is the surface morphology of the leaves. Plants with dense and complex structures result in large unit leaf area, allowing them to deposit more microplastics[38]. Moreover, finer leaf structures lead to larger Stokes coefficient (St), which enhances the capture efficiency of atmospheric particulate matter[39]. For instance, hairy leaf surfaces act as barriers, helping to capture more particulate matter, including microplastics[40]. Another critical factor is electrostatic interaction, which enables deposited microplastics to adhere firmly to the cellulose components of plants[41]. The tufted and fine leaf structure of plant SL provides a larger surface area, resulting in a relatively higher interception efficiency compared to plant RR (Fig. S3). Additionally, biofilms on leaf surfaces may also play a role in microplastic capture, although this requires further investigation.

The planting soil layer is the dominant home for microplastics in green roof modules, primarily through mechanical retention and colloid adsorption. It accounts for more than 66.2% of the total microplastics captured (Fig. 5a). The vertical migration of microplastics within this layer is influenced by the soil's porosity and the physicochemical properties of the microplastics themselves. A previous study has shown that the surface hydrophobicity of microplastics is strongly and positively correlated with their mobility; smaller microplastic particles and larger soil diameters facilitate greater infiltration depth[42]. Additionally, frequent wet-dry cycles promote the vertical migration of microplastics within the soil, leading to a more uniform distribution across different depths as the pore structure becomes more ordered with these cycles[42]. In this study, increased rainfall simulations suggest an increase in wet-dry cycles, contributing to deeper microplastic migration. However, this impact is potentially limited by the relatively shallow soil depth of the green roof module.

The plant roots within the soil layer also play an important role. The growth and decay of roots create cracks that can lead to preferential flow paths for stormwater and associated microplastics[29]. Treatment RR presents a slightly higher interception rate of microplastics than SL (Fig. 2a), mainly attributing to its relatively higher moisture content and lower hydraulic gradient (Fig. 3a), which create more resistances for migration.

Over time, the continuous accumulation of microplastics in green roof substrates may lead to saturation effects, potentially compromising filtration efficiency and even causing secondary release. As MPs accumulate, fragmented particles might clog the porous structure of the substrate[30], altering stormwater infiltration pathways and reducing retention capacity. Additionally, extreme weather conditions, such as prolonged droughts, may destabilize retained MPs, potentially facilitating their re-release.

To mitigate these risks, periodic maintenance of green roofs should be considered. Key design parameters, including media type, filter depth, vegetation type, and system sizing, substantially influence clogging[43], and their appropriate implementation may help maintain long-term MPs interception efficiency. A relatively quick and effective approach is substrate replacement; however, proper disposal of the removed substrate remains a challenge. To achieve a more sustainable solution, introducing invertebrates such as earthworms into the green roof ecosystem could provide a natural remediation strategy. A previous study has reported that earthworms can ingest and degrade MPs in soil, potentially alleviating clogging risks[44]. Furthermore, *Tenebrio molitor* larvae has been shown to fragment and mineralize MPs, with their gut microbiota playing a crucial role in MP degradation[45]. Future research should assess the feasibility of these biological strategies in green roof applications, providing an innovative and eco-friendly approach to managing long-term MP accumulation.

The isolation filter layer contributed minimally to microplastics interception, accounting for just 0–0.03% of the total captured particles (Fig. 5a). This limited effectiveness is likely due to the use of a stainless-steel mesh with pore sizes larger than the microplastics being filtered. Typically, nonwoven fabrics made from synthetic fibers such as polypropylene (PP) and polyester (PET) are used for isolation filter layers in green roof modules. Given this, it is advisable to consider using non-plastic materials with smaller pore sizes for the isolation filter layer in green roofs. Such materials could improve the interception efficiency of microplastics while reducing the risk of contributing to additional microplastic pollution. This approach would enhance the environmental benefits of green roofs by both capturing airborne microplastics and minimizing potential sources of microplastic generation.

The drainage aquifer in this study contributed 1.1–2.4% of the total microplastics captured, a much lower contribution compared to that of the planting soil layer (Fig. 5a). Common drainage aquifer materials include ceramic granules, dimpled plastic drainage boards, and gravels. While these materials generally have a limited impact on retention efficiency in green roofs[46,47], choosing non-plastic materials with a porous structure, such as activated carbon could enhance the adsorption and retention of microplastics. This improvement is due to their higher specific surface area, which can facilitate better capture and containment of microplastics within the drainage layer.

By prioritizing such materials, green roofs can potentially increase their efficiency in trapping microplastics, thus contributing more effectively to reducing microplastic pollution in urban environments.

The amount of microplastics classified as "others" was determined by first calculating the total MPs retained in the system, which is obtained by subtracting the outflow MPs from the inflow MPs. Then, by subtracting the MPs retained in different green roof components from the total retained MPs, the remaining fraction was classified as "others". Although we did not directly measure resuspension, considering that the atmosphere is an important transport pathway for MPs, it is reasonable to assume that some deposited MPs could re-enter the air. A previous study has also confirmed that atmospheric MPs undergo a dynamic process of deposition and resuspension, where the aerodynamic properties of MP particles influence their likelihood of becoming resuspended[48]. The proportion of "others" was calculated to be between 4.3% and 7.9% of the total microplastics, with fibers showing a substantially higher proportion (Fig. 5a). This phenomenon can be attributed to the unique characteristics of fibers compared to other forms of microplastics such as fragments.

Fibers have a larger specific surface area, making them more susceptible to disturbances like air turbulence. As a result, they are more likely to be re-suspended from leaf surfaces and become airborne again. This increased susceptibility to disturbance leads to a relatively higher loss of fiber microplastics compared to other types like fragments. Understanding this dynamic is important for assessing the effectiveness of green roofs and vegetation in capturing and retaining different types of microplastics, and it highlights the need for strategies that minimize re-suspension and enhance retention.

Potential self-generation of microplastics from green roof components

In green roof modules, some components like filter fabrics are often made from polypropylene (PP) due to their construction convenience and cost-effectiveness. However, these plastic components can undergo both biotic and abiotic aging processes, leading to the release of microplastics. To assess the potential risk of microplastic self-generation, two PP sheets of identical dimensions were pre-buried in the soil layer of each treatment. Scanning electron microscopy (SEM) analysis (Fig. 6a) revealed notable changes in the surface morphology of the buried sheets, showing cracks and holes compared to the pristine sheets. The PP sheets buried in the planted treatments

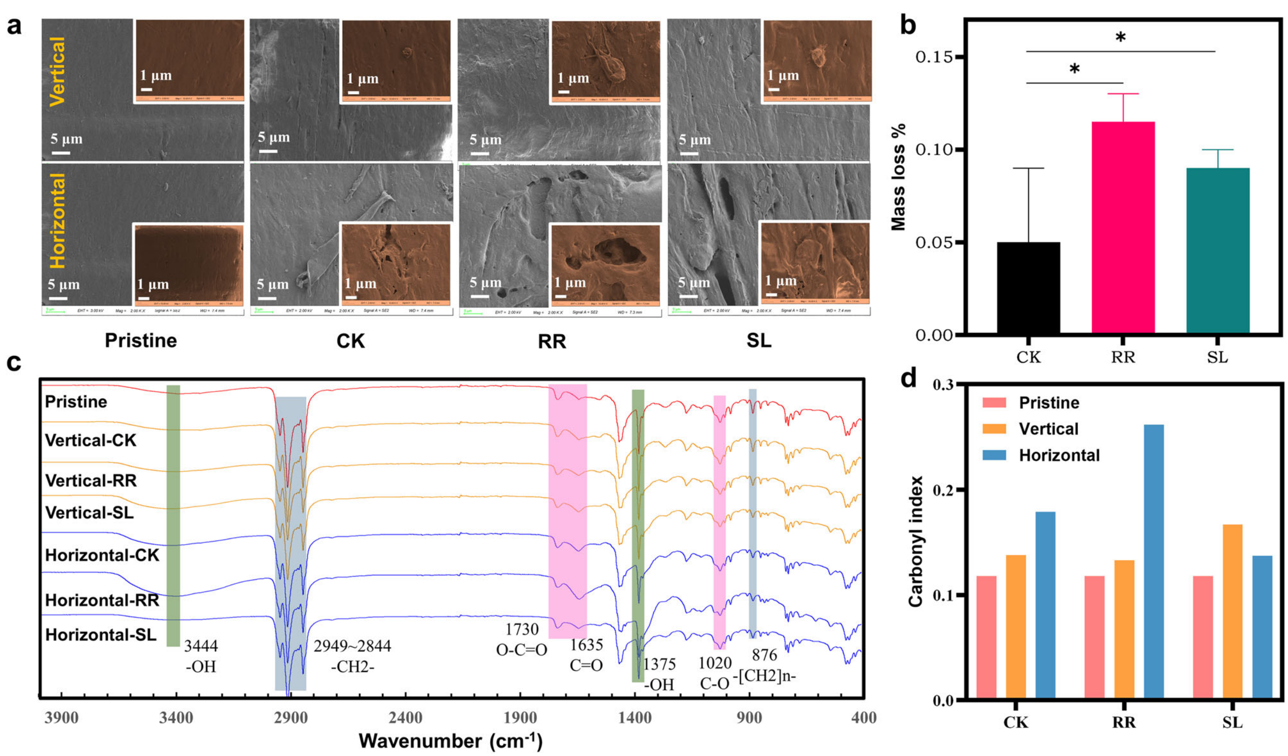

Fig. 6 | Changes in surface characteristics of the pre-buried polypropylene (PP) sheets in green roofs after prolonged use. **a** Surface morphology via scanning electron microscope (SEM). **b** Mass loss of PP sheets. **c** Surface molecular fingerprint via attenuated total reflectance infrared spectrometer (ATR-IR). **d** Calculated carbonyl index. Error bars represent the standard deviation of triplicate measurements.

(RR and SL) exhibited more pronounced aging than those in the control treatment (CK). This was further evidenced by the mass loss observed at the end of the experiment, with planted treatments showing higher mass loss (0.12% for RR and 0.09% for SL) compared to treatment CK (0.05%) (Fig. 6b). This indicates more severe degradation in the presence of plants.

Plastic degradation in natural environments can occur through various processes, including photodegradation, oxidative degradation, and biodegradation[49]. In the context of green roof modules, the buried PP sheets were subjected to dry-wet cycles, which mechanically fragmented them through hydraulic shear forces. Soil microorganisms may also contribute to the breakdown of plastic fragments into smaller particles over time[50]. The higher moisture content in the planted treatments (Fig. 3a) likely resulted in greater hydraulic shear forces, contributing to more significant fragmentation. Additionally, the richer microbial composition in these treatments promoted further degradation. Consequently, mechanical shearing and microbial degradation collectively led to more holes and cracks on the surfaces of the buried PP sheets. The study also found that horizontally buried sheets experienced more severe aging than vertical ones, likely due to their greater contact area with hydraulic shear forces. This highlights the potential for increased microplastic generation from PP components in green roofs, especially in planted environments, and underscores the importance of considering material selection and design to minimize such risks.

FT-IR analyses were performed to further investigate the surface characteristic evolutions from a molecular perspective of buried PP sheets. The FT-IR spectra (Fig. 6c) showed an increase in the transmittance of peaks associated with oxygen-containing functional groups. Notably, the intensities of the hydroxy group (–OH, 3444 cm^{-1}) and carbonyl group (C=O, 1635 cm^{-1}) peaks were particularly enhanced on the surfaces of horizontally buried sheets, indicating a higher level of oxidation. The presence and intensity of oxygen-containing groups, especially the carbonyl group C=O, are widely recognized as indicators of plastic aging. These groups correlate positively with the fragmentation of bulk plastics and the generation of microplastics[51]. The aging process of plastic rainwater facilities is often accompanied by the formation of C=O groups and the breakdown of carbon chains[49], aligning with the observed FT-IR spectrum variations for the horizontally buried sheets. This molecular-level oxidation likely explains the increased surface morphology changes, such as the holes and cracks observed in Fig. 6a.

To quantify the degree of oxidation, the carbonyl index was calculated. Figure 6d shows that the carbonyl indexes ranged from 0.14 to 0.26 for horizontally buried sheets and from 0.13 to 0.17 for vertically buried sheets, both higher than the pristine sheets' index of 0.12. This increase indicates that the buried PP sheets underwent oxidation within the green roof modules, which may lead to fragmentation into microplastics over time. Such ageing and fragmentation within green roofs would be aggravated and be a big challenge for stormwater management, particularly during long-term operations. This underscores the importance of selecting non-plastic materials for future green roof constructions to mitigate the risks associated with microplastic generation and ensure more sustainable stormwater management solutions.

Conclusion

This study highlights the promising potential of green roofs in mitigating microplastic pollution in coastal urban areas. Green roofs demonstrated an impressive average interception efficiency of more than 97.5% for trapping microplastics from atmospheric deposition. The estimated annual interception flux of atmospheric microplastics in Shanghai is 1.70×10^{12} n L^{-1} (56.2 t yr^{-1}). The research found that higher rainfall intensities slightly increased interception efficiency due to enhanced moisture content and reduced hydraulic gradient, decreasing the driving force for stormwater and microplastic infiltration. Fibers were more challengeable to be captured than fragments. Most microplastics were retained in the planting soil layer (66–92%), with the overground part of vegetation contributing modestly. However, the long-term operation of green roofs may lead to aging and degradation of plastic components, potentially generating new microplastics. These findings offer valuable insights and data for developing future microplastic pollution management strategies.

Methods

Construction and operation of green roof

A total of four groups were designed as shown in Table S1 and Fig. S4, including a blank group (BL), a control group (CK), and two experimental groups (RR and SL). The BL group simulated a traditional roof configuration using an empty polypropylene (PP) box (500 mm × 500 mm × 85 mm) without a green roof module. The CK group contained a green roof module but without plants, serving as a control. The RR and SL groups were experimental green roofs, planted with *Rhodiola rosea* (RR) and *Sedum lineare* (SL), respectively—both common green roof species in Shanghai, China. These plants, with stem heights of 10–20 cm, were planted at 50 mm spacing.

All setups included a rainfall generator, a collector, and a green roof module (except for BL) (Fig. 7). The green roof modules were contained within PP boxes and placed at a 0° inclination (completely horizontal) to simulate typical extensive green roof installations in urban settings. Each module consisted of multiple layers. The planting soil was composed of a mix of bio-organic fertilizer, peat perlite, vermiculite, and fermented alcohol, with a layer thickness of 40 mm. For the isolation filter layer, a stainless-steel wire mesh (150 mesh, 109 μm pore size) was used to avoid microplastic interference from aging materials. The drainage aquifer consisted of graded gravel (1–1.5 cm) with a 20 mm depth. Both the gravel and wire mesh were thoroughly rinsed with high-pressure water to prevent microplastic contamination.

To simulate rainfall, a peristaltic pump was used to deliver water to a distributor system composed of pipelines and syringes with stainless-steel needles. These needles, arranged in a checkerboard pattern with 40 mm

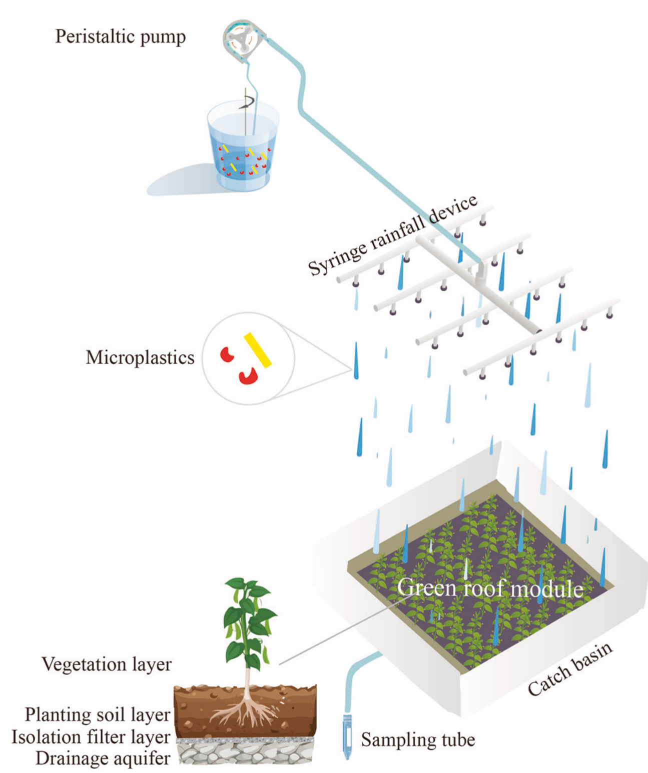

Fig. 7 | Schematic of the experimental setup. A total of four groups were designed, including a blank group (BL, without green roof module), a control group (CK, non-planted), and two planted groups (RR and SL). The CK, RR, and SL groups each consisted of a rainfall generator, a green roof module, and an effluent collector.

spacing, ensured uniform distribution of artificial rainfall. Details of the rainfall device parameters can be found in Table S2. A collector positioned beneath the green roof module collected water samples through the catchment box.

Before starting the experiments, each green roof module underwent a 30-day stabilization period, during which they were watered every 4–5 days using tap water. Subsequently, simulated rainfall events were introduced every 3 days. The study employed four types of rainfall events (light, moderate, heavy, and torrential) classified by intensity (2.5, 7.0, 14.5, and 36.5 mm h^{-1}, respectively), with each event repeated three times and lasting 1–2 h per feeding. Specific rainfall parameters are detailed in Table S3.

Microplastic preparation

The deposition flux of microplastics in Shanghai, China was reported to be 469–12611 n m^{-2} d^{-1}[22]. Our annual monitoring data, obtained from a one-year field study on atmospheric MP deposition in Shanghai in 2021, showed a similar flux (44–15801 n m^{-2} day^{-1}). To convert these deposition fluxes into particle number concentrations, rainfall depth was considered. For instance, using a rainfall depth of 5 mm (as specified in Table S3), the maximum concentration of microplastics was calculated to be 9481 n L^{-1}. The formula is as follows:

$$C_{In} = \frac{Q_{max} \times t}{h} \tag{1}$$

where C_{In} represents the MPs concentration in inflow (n L^{-1}), Q_{max} is the maximum deposition flux (15,801 n m^{-2} day^{-1}), t is the antecedent dry period (3 days), and h is the rainfall depth (5 mm, i.e., 5 L m^{-2}). Based on this formula, the calculated C_{In} value is 9481 n L^{-1}. For simplicity, we adopted a rounded value of 10,000 n L^{-1}, which remains within a reasonable range of environmental concentrations. Consequently, a concentration of 10,000 n L^{-1} was used as the feeding concentration for microplastics in the experiments. In the actual measurements, the average concentration of microplastics in the effluent water from the blank group was found to be 7719 n L^{-1}. This data serves as a baseline for comparison against the green roof treatments.

Two types of microplastics were utilized in the study: rubber in fragment form and polyurethane (PU) in fiber form. These microplastics were derived from their respective plastic products. Detailed information about the raw materials, including infrared spectra and optical microscope images, is provided in Fig. S5. The preparation process for fragmented rubber microplastics involved crushing the raw rubber material into a fine powder using a pulverizer. The powder was then passed through a series of stainless-steel sieves (50, 100, and 150 mesh). The fraction retained on the 150-mesh-sieve (109 μm) was collected and preserved for use in the experiments. For fiber microplastics, PU threads were separated and cut into microfibers using a dissecting shear. The particle size distribution of these prepared microplastic samples (with 90% of particles ranging from 10 to 150 μm) was consistent with the size distribution observed for atmospheric microplastics, where 58.0–76.0% of particles are smaller than 500 μm[22].

This comprehensive setup and preparation ensure that the experimental conditions are reflective of realistic environmental scenarios, facilitating an accurate assessment of the effectiveness of green roofs in managing microplastic pollution.

Sampling and detection methods

Soil moisture content of the control and experimental groups was measured and recorded using a soil moisture meter (ML3, Hualizhen, China).

Outflow water samples: For each simulated rainfall event, outflow water samples were collected at specific time intervals—0, 10, 20, 35, 50, 70, 90, and 110 min after the outflow began. A 100 mL effluent sample was collected at each interval to analyze the presence and characteristics of microplastics. Once collected, the water samples were sent to the laboratory, where they were processed by pumping through and filtering onto GF/F filter membranes with a pore size of 0.45 μm and a diameter of 47 mm. These membranes were then preserved in capped transparent petri dishes with a diameter of 55 mm for further analysis. The particulate matter on the filter membrane was examined using an optical microscope (Olympus BX53, Japan) to document its color and morphological characteristics. Microplastic fragments, identified as red and opaque with distinct irregular edges, and fibers, characterized as yellow, transparent, and clustered with a consistent diameter, were captured in photographs. Identification was further refined using a μ-FTIR laser infrared imaging spectrometer (Agilent 8700 LDIR, USA), applying a database matching threshold of 70%. All identified microplastic fragments and fibers were subsequently photographed with a microscope camera for detailed particle analysis and quantification using ImageJ software (National Institutes of Health, USA).

The spatial distribution of microplastics within the green roof module was assessed by identifying and quantifying the accumulated microplastics in each layer using μ-FTIR spectroscopy and ImageJ software. At the conclusion of the four simulated rainfall experiments, three samples, each measuring 6.0 cm × 6.0 cm, were collected from each layer and transported to the laboratory in aluminum foil.

Microplastics in vegetation and root layer: The collected plant samples were wrapped in A4-sized aluminum foil sheets and transported to the laboratory. Under a laminar flow hood, both the plant surfaces and the aluminum foil were sequentially rinsed with ultrapure water. Specifically, plant leaves stems, and roots were first rinsed three times to remove attached particles, followed by the aluminum foil surfaces. The rinse water was then filtered using GF/F filters (0.45 μm) and stored in transparent Petri dishes (55 mm in diameter) for subsequent analysis. Additionally, after rinsing, plant samples were evenly spread on the aluminum sheet and scanned with an ultra-stereoscopic scanner to detect any missed particles.

Microplastics in soil layer: The green roof module was divided into a 3 × 3 grid (16 cm spacing), and three diagonal grid cells were selected for sampling. Within each selected grid cell, a 6 cm × 6 cm area at the center was designated as the sampling region. Soil from this area was collected using a stainless-steel spatula and placed into a single glass container, where it was thoroughly mixed. Three 10 g subsamples were then taken as replicates for further analysis. Each subsample was suspended in 60 mL of $ZnCl_2$ solution (1.7–1.8 kg L^{-1}) within 100 mL beakers. The mixture was stirred thoroughly for ~10 min and allowed to settle overnight. The resulting suspension was vacuum filtered, and large perlite particles were manually removed with tweezers. Remaining particles underwent a 24-h digestion with 30% H_2O_2 solution in 100 mL beakers to eliminate soil organic matter. The final solution was vacuum filtered (GF/F, 0.45 μm) and stored in transparent Petri dishes (55 mm in diameter).

Microplastics in isolation filter layer: Stainless-steel mesh samples were cut using dissecting scissors, rinsed three times with ultrapure water, and filtered (GF/F, 0.45 μm). The filter membranes were preserved in transparent petri dishes (55 mm in diameter) for further analysis.

Microplastics in drainage aquifer: Gravel samples were rinsed and ultrasonicated in a 500 mL beaker. The solution was then filtered (GF/F, 0.45 μm) and kept in transparent Petri dishes (55 mm in diameter).

Polypropylene (PP) plastic sheets: Polypropylene (PP) plastic sheets, measuring 3 cm × 3 cm × 0.1 cm, were cut from the green roof module and initially weighed (M_0) before being embedded in the planting soil layer at the onset of the experiments. Each green roof module contained two PP sheets: one positioned vertically and the other horizontally. Upon completion of the experiments, the PP sheets were retrieved, rinsed with ultrapure water, and allowed to dry at ambient temperature. The dried sheets were then weighed to obtain their final mass (M_t), and mass loss was calculated by subtracting M_t from M_0. The surface morphology and molecular composition of the PP sheets were analyzed using a scanning electron microscope (SEM, GeminiSEM 300, ZEISS, Germany) and an attenuated total reflectance infrared (ATR-IR) spectrometer (Spectrum TWO, PerkinElmer, USA), respectively.

Quality assurance and quality control

To ensure the reliability of our findings, we implemented rigorous quality assurance and quality control (QA/QC) measures. To prevent airborne contamination, strict contamination control measures were implemented throughout the sampling and analysis process. Specifically, we wore cotton lab coats and nitrile gloves to minimize synthetic fiber shedding. All glassware and tools were thoroughly cleaned with distilled water and ethanol before use, and procedural blanks were included to monitor potential airborne contamination. The ultrapure water used for blanks was obtained from a well-maintained Millipore ultrapure water system to minimize the possibility of contamination. During sampling, blank samples were exposed to the ambient environment at the sampling sites to capture potential airborne contamination. After sampling, they were transported back to the laboratory under the same conditions as the collected samples. During analysis, these blanks were processed using the same filtration, storage, and analytical procedures as the actual samples. Additionally, samples were handled in a laminar flow hood in the laboratory and all open containers were covered with aluminum foil to prevent MP contamination. Replicate samples were analyzed to verify consistency. The accuracy of microplastic identification was validated using certified reference materials and the precision of measurements was maintained through routine calibration of analytical instruments.

Data analysis

The annual interception flux of atmospheric microplastic by green roofs was estimated as follows:

$$Q_n = S_{gr} \times h_{\bar{5}} \times \bar{C}_n \times R_{min} \tag{2}$$

where Q_n is the number-based annual interception flux of microplastics (n yr^{-1}); S_{gr} is the total existing surface area (m^2) of green roofs in Shanghai, China; $h_{\bar{5}}$ is the average annual precipitation (mm yr^{-1}) for the past 5 years in Shanghai; $\bar{C}_n$ is the estimated average microplastic abundance in precipitation (n L^{-1}); and R_{min} is the minimum interception efficiency of green roofs calculated in this study. The interception efficiency (R) was calculated as follows:

$$R = \frac{C_{In} - C_{Out}}{C_{In}} \times 100\% \tag{3}$$

where C_{In} and C_{Out} is the inflow and outflow MP concentrations (n L^{-1}), respectively.

$$Q_g = Q_n \times W_n \tag{4}$$

where Q_g is the weight-based annual interception flux of microplastics (t yr^{-1}). W_n is the average unit weight of microplastic (t n^{-1}), estimated based on the findings of Zhao et al. [23]. Their study measured the mass of microplastic particles within the 60–5000 μm size range, covering 12 identified types of MPs such as polyethylene (PE), polypropylene (PP), and PU. The reported average mass was 0.000033 g n^{-1} (i.e., 3.3×10^{-11} t n^{-1}), which we adopted for our calculations. The mass loss (L) of the pre-buried PP sheets was calculated as follows:

$$L = \frac{M_0 - M_t}{M_0} \times 100\% \tag{5}$$

where L is the mass loss of PP sheets; M_0 is the mass of pristine PP sheets before buried (g); and M_t is the mass of PP sheets sampled after the experiments were finished (g).

Data were recorded and processed using Microsoft Excel (version 2022) and analyzed and visualized using GraphPad Prism (version 9). Shapiro–Wilk test was used to test whether the data were normally distributed. When not normally distributed, a Kruskal–Wallis one-way ANOVA was used to compare differences in interception rates ($\alpha = 0.05$). Two-way ANOVA with Šídák multiple comparisons test was used to determine the P value ($\alpha = 0.05$). Differences were considered significant when the P value was <0.05 and highly significant when the P value was <0.01. The principal component analysis (PCA) and advanced correlation link were performed using R 4.2.2.

Data availability

The source data underlying the main manuscript figures has been deposited in Figshare and is publicly available at: https://doi.org/10.6084/m9.figshare.28954385.v1.

Received: 10 November 2024; Accepted: 22 May 2025;
Published online: 11 June 2025

References

1. Shao, L. et al. Airborne microplastics: a review of current perspectives and environmental implications. *J. Clean. Prod.* **347**, 131048 (2022).
2. Besseling, E., Quik, J. T. K., Sun, M. & Koelmans, A. A. Fate of nano- and microplastic in freshwater systems: a modeling study. *Environ. Pollut. (Barking, Essex: 1987)* **220**, 540–548 (2017).
3. Niu, S., Wang, T. & Xia, Y. Microplastic pollution in sediments of urban rainwater drainage system. *Sci. Total Environ.* **868**, 161673 (2023).
4. He, D. et al. Microplastics in soils: analytical methods, pollution characteristics and ecological risks. *Trends Anal. Chem.* **109**, 163–172 (2018).
5. Brahney, J., Hallerud, M., Heim, E., Hahnenberger, M. & Sukumaran, S. Plastic rain in protected areas of the United States. *Science (New York, NY)* **368**, 1257–1260 (2020).
6. Allen, S. et al. Atmospheric transport and deposition of microplastics in a remote mountain catchment. *Nat. Geosci.* **12**, 339–344 (2019).
7. Choudhury, A. et al. Atmospheric microplastic and nanoplastic: the toxicological paradigm on the cellular system. *Ecotoxicol. Environ. Saf.* **259**, 115018 (2023).
8. Islam, M. S. et al. How microplastics are transported and deposited in realistic upper airways? *Phys. Fluids* **35**, https://doi.org/10.1063/5.0150703 (2023).
9. Bao, M. et al. Microplastics in the atmosphere and water bodies of coastal agglomerations: a mini-review. *Int. J. Environ. Res. Public Health* **20**, https://doi.org/10.3390/ijerph20032466 (2023).
10. Werbowski, L. M. et al. Urban stormwater runoff: a major pathway for anthropogenic particles, black rubbery fragments, and other types of microplastics to urban receiving waters. *ACS EST Water* **1**, 1420–1428 (2021).
11. Yuan, Z. et al. Atmospheric microplastics at a southern China metropolis: occurrence, deposition flux, exposure risk and washout effect of rainfall. *Sci. Total Environ.* **869**, 161839 (2023).
12. Liu, F., Olesen, K. B., Borregaard, A. R. & Vollertsen, J. Microplastics in urban and highway stormwater retention ponds. *Sci. Total Environ.* **671**, 992–1000 (2019).
13. Han, N., Zhao, Q., Ao, H., Hu, H. & Wu, C. Horizontal transport of macro- and microplastics on soil surface by rainfall induced surface runoff as affected by vegetations. *Sci. Total Environ.* **831**, 154989 (2022).
14. Wang, Q., Hernández-Crespo, C., Santoni, M., van Hulle, S. & Rousseau, D. P. L. Horizontal subsurface flow constructed wetlands as tertiary treatment: can they be an efficient barrier for microplastics pollution?. *Sci. Total Environ.* **721**, 137785 (2020).
15. Koutnik, V. S. et al. Microplastics retained in stormwater control measures: where do they come from and where do they go?. *Water Res.* **210**, 118008 (2022).

16. Shafique, M., Kim, R. & Rafiq, M. Green roof benefits, opportunities and challenges—a review. *Renew. Sustain. Energy Rev.* **90**, 757–773 (2018).
17. Hashemi, S. S. G., Mahmud, H. B. & Ashraf, M. A. Performance of green roofs with respect to water quality and reduction of energy consumption in tropics: a review. *Renew. Sustain. Energy Rev.* **52**, 669–679 (2015).
18. Speak, A. F., Rothwell, J. J., Lindley, S. J. & Smith, C. L. Rainwater runoff retention on an aged intensive green roof. *Sci. Total Environ.* **461**-**462**, 28–38 (2013).
19. Stovin, V., Vesuviano, G. & Kasmin, H. The hydrological performance of a green roof test bed under UK climatic conditions. *J. Hydrol.* **414**-**415**, 148–161 (2012).
20. Lee, J. H., Bang, K. W., Ketchum, L. H., Choe, J. S. & Yu, M. J. First flush analysis of urban storm runoff. *Sci. Total Environ.* **293**, 163–175 (2002).
21. O'Connor, D. et al. Microplastics undergo accelerated vertical migration in sand soil due to small size and wet-dry cycles. *Environ. Pollut.* **249**, 527–534 (2019).
22. Jia, Q. et al. Atmospheric deposition of microplastics in the megalopolis (Shanghai) during rainy season: Characteristics, influence factors, and source. *Sci. Total Environ.* **847**, 157609 (2022).
23. Zhao, S. et al. Analysis of suspended microplastics in the Changjiang Estuary: implications for riverine plastic load to the ocean. *Water Res.* **161**, 560–569 (2019).
24. Chen, H. et al. Quantifying microplastic stocks and flows in the urban agglomeration based on the mass balance model and source–pathway–receptor framework: revealing the role of pollution sources, weather patterns, and environmental management practices. *Water Res.* **224**, 119045 (2022).
25. Smyth, K. et al. Bioretention cells remove microplastics from urban stormwater. *Water Res.* **191**, 116785 (2021).
26. Wu, S. et al. The interaction of microplastic and heavy metal in bioretention cell: contributions of water–soil–plant system. *Environ. Pollut. (Barking, Essex: 1987)* **361**, 124853 (2024).
27. Scholl, P. et al. Root induced changes of effective 1D hydraulic properties in a soil column. *Plant Soil* **381**, 193–213 (2014).
28. Armson, D., Stringer, P. & Ennos, A. R. The effect of street trees and amenity grass on urban surface water runoff in Manchester, UK. *Urban For. Urban Green.* **12**, 282–286 (2013).
29. Johnson, M. S. & Lehmann, J. Double-funneling of trees: stemflow and root-induced preferential flow. *Écoscience* **13**, 324–333 (2006).
30. Waldschläger, K. & Schüttrumpf, H. Infiltration behavior of microplastic particles with different densities, sizes, and shapes—from glass spheres to natural sediments. *Environ. Sci. Technol.* **54**, 9366–9373 (2020).
31. Assouline, S. Infiltration into soils: conceptual approaches and solutions. *Water Resour. Res.* **49**, 1755–1772 (2013).
32. Fischer, C. et al. How do earthworms, soil texture and plant composition affect infiltration along an experimental plant diversity gradient in grassland?. *PLoS ONE* **9**, e98987 (2014).
33. Kuoppamäki, K., Lima, S. P., Scopetani, C. & Setälä, H. The ability of selected filter materials in removing nutrients, metals, and microplastics from stormwater in biofilter structures. *J. Environ. Qual.* **50**, 465–475 (2021).
34. Fouli, Y., Cade-Menun, B. J. & Cutforth, H. W. Freeze–thaw cycles and soil water content effects on infiltration rate of three Saskatchewan soils. *Can. J. Soil Sci.* **93**, 485–496 (2013).
35. Liu, H. et al. Effects of rainfall intensity and antecedent soil water content on soil infiltrability under rainfall conditions using the run off-on-out method. *J. Hydrol.* **396**, 24–32 (2011).
36. Liu, Y., Cui, Z., Huang, Z., López-Vicente, M. & Wu, G.-L. Influence of soil moisture and plant roots on the soil infiltration capacity at different stages in arid grasslands of China. *CATENA* **182**, 104147 (2019).
37. Liu, K., Wang, X., Song, Z., Wei, N. & Li, D. Terrestrial plants as a potential temporary sink of atmospheric microplastics during transport. *Sci. Total Environ.* **742**, 140523 (2020).
38. Gutow, L., Eckerlebe, A., Giménez, L. & Saborowski, R. Experimental evaluation of seaweeds as a vector for microplastics into marine food webs. *Environ. Sci. Technol.* **50**, 915–923 (2016).
39. Beckett, K. P., Freer-Smith, P. H. & Taylor, G. Particulate pollution capture by urban trees: effect of species and windspeed. *Glob. Change Biol.* **6**, 995–1003 (2000).
40. Chiam, Z., Song, X. P., Lai, H. R. & Tan, H. T. W. Particulate matter mitigation via plants: understanding complex relationships with leaf traits. *Sci. total Environ.* **688**, 398–408 (2019).
41. Bhattacharya, P., Lin, S., Turner, J. P. & Ke, P. C. Physical adsorption of charged plastic nanoparticles affects algal photosynthesis. *J. Phys. Chem. C***114**, 16556–16561 (2010).
42. Gao, J. et al. Vertical migration of microplastics in porous media: multiple controlling factors under wet-dry cycling. *J. Hazard. Mater.* **419**, 126413 (2021).
43. Le Coustumer, S., Fletcher, T. D., Deletic, A., Barraud, S. & Poelsma, P. The influence of design parameters on clogging of stormwater biofilters: a large-scale column study. *Water Res.* **46**, 6743–6752 (2012).
44. Wang, L. et al. Earthworms' degradable bioplastic diet of polylactic acid: easy to break down and slow to excrete. *Environ. Sci. Technol.* **56**, 5020–5028 (2022).
45. Peng, B.-Y., Xu, Y., Zhou, X., Wu, W.-M. & Zhang, Y. Generation and fate of nanoplastics in the intestine of plastic-degrading insect (*Tenebrio molitor* larvae) during polystyrene microplastic biodegradation. *Environ. Sci. Technol.* **58**, 10368–10377 (2024).
46. Bianchini, F. & Hewage, K. How "green" are the green roofs? Lifecycle analysis of green roof materials. *Build. Environ.* **48**, 57–65 (2012).
47. Scolaro, T. P. & Ghisi, E. Life cycle assessment of green roofs: a literature review of layers materials and purposes. *Sci. Total Environ.* **829**, 154650 (2022).
48. Rao, W., Fan, Y., Li, H., Qian, X. & Liu, T. New insights into the long-term dynamics and deposition-suspension distribution of atmospheric microplastics in an urban area. *J. Hazard. Mater.* **463**, 132860 (2024).
49. Liu, C. et al. Ageing characteristics and microplastic release behavior from rainwater facilities under ROS oxidation. *Sci. Total Environ.* **866**, 161397 (2023).
50. Liu, J. et al. Soil microorganisms play an important role in the detrimental impact of biodegradable microplastics on plants. *Sci. Total Environ.* **933**, 172933 (2024).
51. Almond, J., Sugumaar, P., Wenzel, M. N., Hill, G. & Wallis, C. Determination of the carbonyl index of polyethylene and polypropylene using specified area under band methodology with ATR-FTIR spectroscopy. *e-Polymers* **20**, 369–381 (2020).

Acknowledgements
This work was supported by grants from the National Natural Science Foundation of China (52170168) and the Science and Technology Project of Shanghai Landscape and City Appearance Administrative Bureau (G240202).

Author contributions
Jianshi Huang prepared the draft manuscript text and figures. Mengrong Bao performed the data analysis and contributed to the data collection. Shuangqi Wu assisted in the visualization of data. Ying Wang assisted with data collection. Shuiping Cheng guided the study design and reviewed the paper.

Competing interests
The authors declare no competing interests.

Additional information

Supplementary information The online version contains supplementary material available at https://doi.org/10.1038/s43247-025-02407-w.

Correspondence and requests for materials should be addressed to Shuiping Cheng.

Peer review information *Communications Earth & Environment* thanks Rasa Zalakeviciute and the other, anonymous, reviewer(s) for their contribution to the peer review of this work. Primary Handling Editors: Somaparna Ghosh [A peer review file is available].